

# Phase Stability in 3d-5d (NiPt and CuAu) and 3d-4d (NiPd and CuAg) Systems

Durga Paudyal and Abhijit Mukherjee

S.N. Bose National Centre for Basic Sciences, JD Block, Sector 3, Salt Lake City,  
Kolkata 700098, India

**Abstract.** We show the differences in the stability of 3d-5d (NiPt and CuAu) and 3d-4d (NiPd and CuAg) alloys arise mainly due to relativistic corrections. The magnetic properties of disordered NiPd and NiPt alloys also differ due to these corrections which lead to increase in the separation between s-d bands of 5d elements in these alloys. For the magnetic case we analyze the results in terms of splitting of majority and minority spin d-band centers of the 3d elements. We further examine the effect of relativistic corrections to the pair energies and order disorder transition temperatures in these alloys. The magnetic moments and Curie temperatures have also been studied along with the short range ordering/segregation effects in NiPt/NiPd alloys.

PACS numbers: 71.20, 71.20c

## 1. Introduction

It is well known at the level of standard chemistry that the main chemical difference between pairs of 4d and 5d transition elements is the relativistic contraction of the valence s and p states relative to the d and f states. Recently Wang and Zunger [1] studied ordered 3d-5d (NiPt and CuAu) and 3d-4d (NiPd and CuAg) alloys and pointed out the effect of relativistic corrections in the formation energies in these alloys. In this communication we shall provide a quantitative, electronic structure analysis of these corrections in both ordered as well as disordered phases of these alloys, and demonstrate its consequences on phase stability. We shall show, via a first-principle calculation, that in binary alloys of the late 3d-5d intermetallics, the 3d-5d coupling is dominant. This effect results from the relativistic up-shift of the 5d band, which brings it closer to the 3d band of the other element, significantly enhancing 3d-5d hybridization. In addition, the relativistic s orbital contraction significantly reduces the lattice constant of the 5d element, thus lowering the size mismatch with the 3d element. This reduces the strain energy associated with packing 3d and 5d atoms of dissimilar sizes onto a given lattice. Both the enhanced d-d hybridization and the reduced packing strain are larger in 3d-5d intermetallics than in 3d-4d. This explains why the 3d-5d alloys CuAu and NiPt have

z email: dpaudyal@bose.res.in

x email: abhijit@bose.res.in

negative formation energies and thus form stable ordered alloys, whereas the analogous isovalent 3d-4d alloys CuAg and NiPd, made of elements from the same columns in the periodic table, have positive formation energies and thus either phase separate or remain mostly in disordered phases. Simple arguments, such as atomic size mismatch or electronegativity differences, do not explain these two different behaviours. The constituent elements in the stable NiPt and CuAu alloys have larger atomic size mismatch than the unstable NiPd and CuAg. Likewise, the stable NiPt has a smaller electronegativity difference than unstable CuAg.

Our calculation of pair energies shows that the inclusion of relativistic effect in the electronic structure calculation is often important in order to get the correct ordering behaviour seen experimentally. It is experimentally known that NiPt and CuAu are ordering at low temperatures, CuAg is segregating and NiPd remains disordered but with a tendency toward short-ranged clustering. To obtain the correct ordering tendency for NiPt and CuAu we need to carry out scalar relativistic calculations. For CuAg the non-relativistic calculations do show the correct segregating behaviour. However, scalar relativistic calculations are quantitatively more accurate. For NiPd we have to carry out calculations on the disordered alloy with short-ranged clustering effects included, so as to give the correct magnetic moment per atom.

From experiments the difference in the magnetic properties of disordered NiPd and NiPt alloys does not seem to be obvious as both Pd and Pt have the same number of valence electrons. Earlier works [2, 3, 4] on the magnetic properties of NiPd and NiPt alloys used parametrized local environment models to describe the magnetism in NiPd and NiPt alloys. These models incorporated the changes induced due to the chemical environment as well as the magnetic environment. The present study is intended to improve our understanding of the reasons which lead to differences in the magnetic properties of disordered NiPd and NiPt alloys and determine the effect of chemical, as well as magnetic, environments from a first principles approach. In an earlier communication [5] we have pointed out that environmental effect is important in NiPt alloys and single-site mean field approximations like the coherent potential approximation fail to predict the correct tendency in magnetic moments. In this paper our emphasis is on NiPd, in which we have found that short-ranged segregation in an otherwise disordered alloy actually enhances ferromagnetic behaviour at par with the experimental predictions.

The differences in the magnetic properties of NiPd and NiPt alloys are also dictated by the electronic structure of 4d Pd and 5d Pt atoms and the subsequent hybridization of these states with the d states of Ni atoms. Since relativistic corrections are more important for heavier elements, the differences in the electronic structure of Pd and Pt atoms are mainly due to relativistic effects.

## 2. Theoretical and Computational methods

For ordered structures we have performed the total energy density functional calculations. The Kohn-Sham equations were solved in the local density approximation (LDA) with von Barth-Hedin (vBH) [6] exchange correlations. The calculations have been performed in the basis of tight binding linear mu n-tin orbitals in the atomic sphere approximation (TB-LMTO-ASA) [7]-[10] including combined corrections. Two sets of calculations have been performed one scalar relativistic through inclusion of mass-velocity and Darwin correction terms and another without. The k-space integration was carried out with  $32 \times 32 \times 32$  mesh resulting 2601 k points for tetragonal primitive structures in the irreducible part of the corresponding Brillouin zone. The convergence of the total energies with respect to k-points have been checked.

As we know when the alloy is formed the elemental solids are deformed from their equilibrium lattice constants ( $a_A^0, a_B^0$ ) to the lattice constants ( $a$ ) of the alloy. Therefore in the alloy formation there are two types of formation energies. One is elastic formation energy which is given as:

$$H_{\text{elast}} = x [E_A(a) - E_A(a_A^0)] + (1-x) [E_B(a) - E_B(a_B^0)]$$

and another is chemical formation energy

$$H_{\text{chem}} = E(A_x B_{1-x}; a) - x E_A(a) - (1-x) E_B(a)$$

where  $x$  is the concentration of one of the constituents.

The sum of these formation energies is the conventional alloy formation energy.

$$H = H_{\text{elast}} + H_{\text{chem}} \quad (1)$$

For stability arguments, we start from a completely disordered alloy. Each site  $R$  has an occupation variable  $n_R$  associated with it. For a homogeneous perfect disorder  $\ln_R i = x$ , where  $x$  is the concentration of one of the components of the alloy. In this homogeneously disordered system we now introduce fluctuations in the occupation variable at each site:  $x_R = n_R - x$ . Expanding the total energy in this new configuration about the energy of the perfectly disordered state we get:

$$E(x) = E^{(0)} + \sum_{R=1}^N E_R^{(1)} x_R + \sum_{R,R^0=1}^N E_{RR^0}^{(2)} x_R x_{R^0} + \dots \quad (2)$$

The coefficients  $E^{(0)}, E_R^{(1)}, \dots$  are the effective renormalized cluster interactions.  $E^{(0)}$  is the energy of the averaged disordered medium. The renormalized pair interactions  $E_{RR^0}^{(2)}$  express the correlation between concentration fluctuations at two sites and are the most dominant quantities for the analysis of phase stability. In the series expansion, we will retain terms only up to pair interactions. Higher order interactions may be included for a more accurate and complete description.

The total energy of a solid may be separated into two terms: a one-electron band contribution  $E_{BS}$  and the electrostatic contribution  $E_{ES}$ . The renormalized cluster interactions defined in (2) should, in principle, include both  $E_{BS}$  and  $E_{ES}$  contributions.

Since the renormalized cluster interactions involve the difference of cluster energies, it is usually assumed that the electrostatic terms cancel out and only the band structure contribution is important. Such an assumption which is not rigorously true, has been shown to be approximately valid in a number of alloy systems [11]. Considering only band structure contribution, it is easy to see that the effective pair interactions may be written as :

$$E_{RR^0}^{(2)} = E_{RR^0}^{AA} + E_{RR^0}^{BB} - E_{RR^0}^{AB} - E_{RR^0}^{BA} \quad (3)$$

We have computed these pair energies using augmented space recursion with the TB-LMTO Hamiltonian coupled with orbital peeling which allows us to compute configuration averaged pair-potentials directly, without resorting calculations involving small differences of large total energies. The details of this method is given in our previous paper [12] and the references therein.

For the calculation of order disorder transition temperature we have used Khachatryan's concentration wave approach in which the stability of a solid solution with respect to a small concentration wave of given wave vector  $\mathbf{k}$  is guaranteed as long as  $k_B T + V(\mathbf{k})c(1-c) > 0$ . Instability of the disordered state sets in when :

$$k_B T^i + V(\mathbf{k})c(1-c) = 0 \quad (4)$$

$T^i$  is the instability temperature corresponding to a given concentration wave disturbance.  $V(\mathbf{k})$  is the Fourier transform of pair energies and  $c$  is the concentration of one of the constituent atoms. The details are given in our previous paper [12] and references therein.

The antiphase boundary energies between  $L1_0$  and  $L1_2$  structures and their corresponding superstructures  $A_2B_2$  and  $D0_{22}$  [13] are :

$$= -V_2 + 4V_3 - 4V_4 ; \quad (5)$$

for  $c > 0$   $L1_2$  and  $L1_0$  are the stable structures at concentration 25 % and 50 % while for  $c < 0$ , the stable superstructures are  $D0_{22}$  and  $A_2B_2$ .

Orbital magnetic calculations are based on the generalized ASR technique [5],[14]--[18]. The Hamiltonian in the TB-LMTO minimal basis is sparse and therefore suitable for the application of the recursion method introduced by Haydock et al [19]. The ASR allows us to calculate the configuration averaged Green functions. It does so by augmenting the Hilbert space spanned by the TB-LMTO basis by the configuration space of the random Hamiltonian parameters. The configuration average is expressed exactly as a matrix element in the augmented space. A generalized form of this methodology is capable of taking into account the effect of short range order. Details are given in our previous [5] paper and references therein.

For the treatment of the Madelung potential, we follow the procedure suggested by Kudmovsky et al [20] and use an extension of the procedure proposed by Andersen et al [7]. We choose the atomic sphere radii of the components in such a way that they preserve the total volume on the average and the individual atomic spheres are almost charge neutral. This ensures that total charge is conserved, but each atomic sphere

carries no excess charge. In doing so, one needs to be careful about the sphere overlap which should be under certain limit so as to not violate the atomic sphere approximation.

To calculate the Curie temperature  $T_C$  we have used the Mohn-Wolfarth (MW) procedure [21] :

$$\frac{T_C}{T_S}^2 + \frac{T_C}{T_{SF}} - 1 = 0$$

where,  $T_S$  is the Stoner temperature calculated from the relation

$$hI(E_F)i \int_{-1}^1 dE N(E) \frac{\partial f}{\partial E} = 1$$

$hI(E_F)i$  is the concentration averaged Stoner parameter,  $N(E)$  is the density of states per atom per spin of the paramagnetic state [22] and  $f(E)$  is the Fermi distribution function. The spin fluctuation temperature  $T_{SF}$  is given by,

$$T_{SF} = \frac{m^2}{10k_B h_0 i}$$

$h_0 i$  is the concentration weighted exchange enhanced spin susceptibility at equilibrium and  $m$  is the averaged magnetic moment per atom.  $h_0$  is calculated using the relation by Mohn [21] and Gersdorf [23]:

$$h_0^{-1} = \frac{1}{2 \chi_B} \left[ \frac{1}{2N^+(E_F)} + \frac{1}{2N^-(E_F)} \right] I$$

$N^+(E_F)$  and  $N^-(E_F)$  are the spin-up and spin-down partial density of states per atom at the Fermi level for each species in the alloy.

In these calculations one also needs to be very careful about the convergence of our procedure. Errors can arise in the augmented space recursion because one can carry out only finite number of recursion steps and then terminate the continued fraction using available terminators. We ensure that the recursion is carried out for sufficient number of steps so that the errors in Fermi energy, moments of the density of states and magnetic moment remain within a prescribed window.

The formulation of the augmented space recursion used for the calculation in the present paper is the energy dependent augmented space recursion in which the disordered Hamiltonian with diagonal as well as off-diagonal disorder is recast into an energy dependent Hamiltonian having only diagonal disorder. We have chosen a few seed points across the energy spectrum uniformly, carried out recursion on those points and spline fit the coefficients of recursion throughout the whole spectrum. This enabled us to carry out large number of recursion steps since the configuration space grows significantly less faster for diagonal as compared with off-diagonal disorder. Convergence of physical quantities with recursion steps have been discussed in detail earlier by Ghosh et al [24, 25].

Table 1. Formation energies in mRyd/atom. The values shown in the brackets are without relativistic corrections.

Alloy system	$H_{\text{form}}$	$H_{\text{elastic}}$	$H_{\text{chemical}}$
NiPd (this work)	3.54 (5.38)	17.05 (18.13)	-13.51 (-12.75)
Wang and Zunger [1]	3.63 (6.22)	19.83 (21.05)	-16.20 (-14.83)
NiPt (this work)	-9.17 (4.44)	22.22 (31.48)	-31.39 (-27.04)
Wang and Zunger [1]	-6.26 (8.17)	29.74 (40.38)	-36.00 (-32.21)
CuAg (this work)	6.21 (8.13)	16.30 (17.49)	-10.09 (-9.36)
Wang and Zunger [1]	7.51 (9.34)	18.74 (19.66)	-11.23 (10.32)
CuAu (this work)	-5.97 (10.72)	19.20 (28.99)	-25.17 (-18.27)
Wang and Zunger [1]	-3.64 (12.16)	27.43 (35.13)	-31.07 (-22.97)

### 3. Results and Discussion

#### 3.1. Calculations on ordered alloys

3.1.1. Formation energies : In table 1, we show the calculated formation energies of the  $L1_0$  structure of NiPd, NiPt, CuAg and CuAu alloys calculated relativistically (including mass velocity and Darwin correction but without spin orbit couplings) as well as non-relativistically. The calculations were performed taking the same lattice parameters that were calculated by Wang and Zunger [1] and shown in their paper. The relativistically calculated formation energies (in mRyd/atom) are 3.54, -9.17, 6.21 and -5.97 for NiPd, NiPt, CuAg and CuAu. We see the clear ordered alloy formation trend of CuAu and NiPt as contrasted with the phase-separating or disordering trend of CuAg and NiPd. To gain better insight into those trends, we have decomposed the total formation energies into chemical formation energy and elastic formation energy. The elastic energy of formation is the energy needed to deform the elemental solids A and B from their respective equilibrium lattice constants and to the lattice constants of the  $AB$  alloy. Since a deformation of equilibrium structures is involved, the chemical energy of formation is simply the difference between the (fully relaxed) total energy of the alloy and the energies of the deformed constituents. In general the elastic formation energy is positive and that of chemical formation energy is negative. The sum gives the conventional definition of alloy formation energy and the system is stable only if this formation energy is negative. This clearly shows lower the volume-deformation energy of the constituents enhances the (negative) chemical formation energy giving rise to the possibility of forming a stable ordered alloy.

Table 1, shows that the relativistic effect significantly reduces the elastic energy of formation of 3d-5d alloys (e.g. from 31.48 to 22.22 mRyd/atom in NiPt and from 28.99 to 19.20 mRyd/atom in CuAu). This effect is much smaller in the 3d-4d systems (e.g. from 18.13 to 17.05 mRyd/atom in NiPd and 17.49 to 16.30 mRyd/atom in CuAg). The reason for this can also be appreciated by inspecting the non-relativistically-and

Table 2. Band centres (eV) in Ryd/atom. The values shown in the brackets are without relativistic corrections.

Alloy system	Site (A/B)	s orbital	p orbital	d orbital
NiPd	Ni	-359.0 (-343.6)	676.3 (650.5)	-217.1 (-228.0)
	Pd	-317.6 (-240.8)	746.2 (763.1)	-321.9 (-335.0)
NiPt	Ni	-349.4 (-347.2)	707.0 (641.4)	-210.5 (-227.9)
	Pt	-524.0 (-283.8)	642.1 (694.0)	-324.8 (-366.3)
CuAg	Cu	-441.9 (-423.3)	524.9 (503.6)	-315.5 (-328.2)
	Ag	-423.5 (-362.9)	539.4 (529.6)	-481.6 (-511.6)
CuAu	Cu	-436.1 (-426.4)	550.6 (492.9)	-307.6 (-326.8)
	Au	-597.1 (-394.5)	485.6 (471.9)	-456.6 (-536.2)

relativistically-calculated equilibrium lattice constants of the fcc elements as already shown by Wang and Zunger [1].

In addition to reduction in the (positive) elastic energy of formation, table 1 also shows that relativistic corrections enhance the (negative) chemical energy of formation (e.g. from -27.04 to -31.39 mRyd/atom in NiPt and from -18.27 to -25.17 mRyd/atom in CuAu). This effect is much smaller in 3d-4d alloys (e.g. from -12.75 to -13.51 mRyd/atom in NiPd and from -9.36 to -10.09 mRyd/atom in CuAg). There are two effects that explain this relativistic chemical stabilization. First the relativistic raising of the energy of the 5d state reduces the 3d-5d energy difference and thus improve the 3d-5d bonding; second the relativistic lowering the s bands and raising of the d band leads to an increased occupation of the bonding s bands and a decreased occupation of the anti-bonding d band. These effects can be appreciated by band centres shown in table 2 from which we can see that the 5d and 3d bands are closer to each other in the relativistic limit than in the non-relativistic limit and play important role for formation energies in these alloys. From table 3, it is seen that the difference in hopping integrals between 3d and 5d are higher than 3d and 4d in relativistic case which is the signature of higher overlap and hence the stability in NiPt and CuAu alloys with relativistic corrections. The larger 3d-5d overlap in relativistic NiPt than in relativistic CuAu may also explain the more negative formation energy in NiPt than in CuAu. The d-d interaction from different sublattices in late d alloy plays a key role. Relativity results in the raising of the energy of the 5d band (bringing the 5d band closer to the 3d band) and in a large charge-transfer from the anti-bonding edge of the 5d band to the bonding 6sp bands thus enhancing the chemical stability of the 3d-5d alloys.

Our results for formation energies are comparable, within the error window of our calculational method, to the results obtained by Wang and Zunger [1]. These authors used full potential linearized augmented plane wave method with exchange correlation functional of Ceperley and Alder parametrized by Perdew and Zunger [1]. They have carried out k space integration with  $8 \times 8 \times 8$  mesh resulting 60 special k points. On the

Table 3. Hopping integrals (eV) mRyd/atom. The values shown in the brackets are without relativistic corrections.

Alloy system	Site (A/B)	s orbital	p orbital	d orbital
NiPd	Ni	176.1 (172.6)	155.9 (152.7)	9.9 (9.4)
	Pd	182.3 (184.8)	186.7 (184.3)	22.7 (21.1)
NiPt	Ni	177.6 (167.6)	151.5 (142.8)	9.4 (8.4)
	Pt	163.6 (175.0)	186.4 (183.4)	29.8 (25.5)
CuAg	Cu	153.6 (150.1)	138.2 (133.7)	7.2 (6.6)
	Ag	157.4 (157.4)	163.9 (160.0)	15.7 (14.0)
CuAu	Cu	156.0 (145.1)	136.8 (124.8)	7.0 (5.9)
	Au	144.0 (149.1)	166.7 (158.9)	22.2 (17.3)

other hand we have in our TB-LMTO calculation used von Barth and Hedin exchange correlation functional and we have carried out the  $k$  space integration with  $32 \times 32 \times 32$  mesh resulting 2601 special  $k$  points to ensure the convergence of total energy.

3.1.2. Separation between  $s$  and  $d$  band centres : It is seen that the phase stability in 3d-5d alloys are brought by relativity through its effect on heavier atoms. We know that the most dominant effect of relativity is to lower the  $s$  potential. From table 2 it is clearly seen that the energy band centre of Pt in NiPt and Au in CuAu is lower in relativistic case than in non relativistic case. The lowering of  $s$  potential causes (i) the  $s$ -wavefunction to contract leading to a contraction of the lattice, and increased  $s$ - $d$  hybridization which results in electron transfer from  $d$  to  $s$ . We see that the change in  $s$ - $d$  separation is more in Pt and Au in NiPt and CuAu alloys than in Pd and Ag in NiPd and CuAg alloys. The  $s$ - $d$  separation for Pd in NiPd alloy changes from 94.3 mRy to 4.3 mRy, whereas for Pt in NiPt alloy, it changes from 82.5 mRy to -199.2 mRy. Similarly the  $s$ - $d$  separation for Ag in CuAg alloy changes from 148.8 mRy to 58.1 mRy, whereas for Au in CuAu alloy, it changes from 141.7 mRy to -140.5 mRy. Thus the contraction of the  $s$  wavefunction of Pt and the subsequent  $s$ - $d$  hybridization must be responsible for reducing the size mismatch and hence reduces the strain in NiPt and CuAu alloys giving rise to the stable structures.

### 3.2. Calculations on disordered alloys

3.2.1. Effective pair energies : In table 4, we show the effective pair energies up to fourth nearest neighbour in 3d-4d NiPd, CuAg and 3d-5d NiPt, CuAu alloys.

The first nearest neighbour pair interaction in NiPt shows ordering behaviour. Indeed, with the relativistic correction, the antiphase boundary energy indicates a stable ordered  $L1_0$  low temperature phase. The formation energy of the  $L1_0$  phase is negative, confirming stability. However, all these results are true only with the inclusion of relativistic corrections.



Table 4. Pair energies in mRyd/atom. The values shown in the brackets are without relativistic corrections.

Alloy system	v1	v2	v3	v4
NiPd	5.16 (4.56)	0.02 (-0.16)	0.05 (0.09)	0.07 (0.09)
NiPt	10.08 (10.11)	0.10 (0.13)	0.01 (0.25)	-0.24 (0.17)
CuAg	-0.63 (-0.90)	0.09 (0.05)	-0.02 (0.00)	0.12 (0.10)
CuAu	2.29 (-0.23)	0.19 (0.20)	0.06 (0.11)	0.21 (0.17)

For NiPd we have a problem. Although the positive nearest neighbour pair interaction indicates ordering tendency, even with relativistic correction, the antiphase boundary energy and the formation energies indicate that the ordered structure is not stable at low temperatures. This same remains true even if we include magnetic effects in the pair interaction. This alloy remains disordered in low temperatures. However, whether this is because of the fact that at low temperatures the atomic mobilities are too low for ordering to proceed fast (as in AgPd, for example), one cannot say with certainty.

The first nearest neighbour pair interaction of CuAg shows segregation behaviour which matches with the positive value of formation energy of the ordered calculations.

In CuAu alloy the pair interaction calculations without relativistic correction shows segregation tendency. Inclusion of these corrections lead to the correct conclusion of an ordering behaviour. Our relativistic calculation in ordered CuAu shows that the with  $L1_0$  structure has lower total energy than the  $A_2B_2$  superstructure. This confirms a stable  $L1_0$  low temperature structure of CuAu. However, the antiphase boundary energy has the wrong sign. This could be due to the fact that in CuAu the APB energies are long ranged and more than the fourth nearest neighbour values need to be taken.

3.2.2. Order disorder transition temperatures : Using these pair interactions obtained by us, we have calculated the instability temperatures in NiPt and CuAu alloys with relativistic corrections. For the entropy part we have taken a simple mean-field Bragg-Williams expression. The calculated instability temperature in NiPt comes out to be 1683°K which is higher than the experimental estimate which was discussed in great detail in our previous paper [12]. Our calculation in CuAu alloy shows an instability temperature (246°K) slightly higher than the experimental estimate (137°K). The Bragg-Williams tends to overestimate the transition temperature, consistent with our results.

Our calculations (with relativistic corrections) indicate that order disorder transition takes place in NiPd at around (812°K) is slightly higher than the non relativistic one (743°K). Since there is no experimental evidence of order disorder transition in this system, we only comment that this system mainly tends to remain in a disordered phase. Looking at the high value (457°K) of the experimental Curie

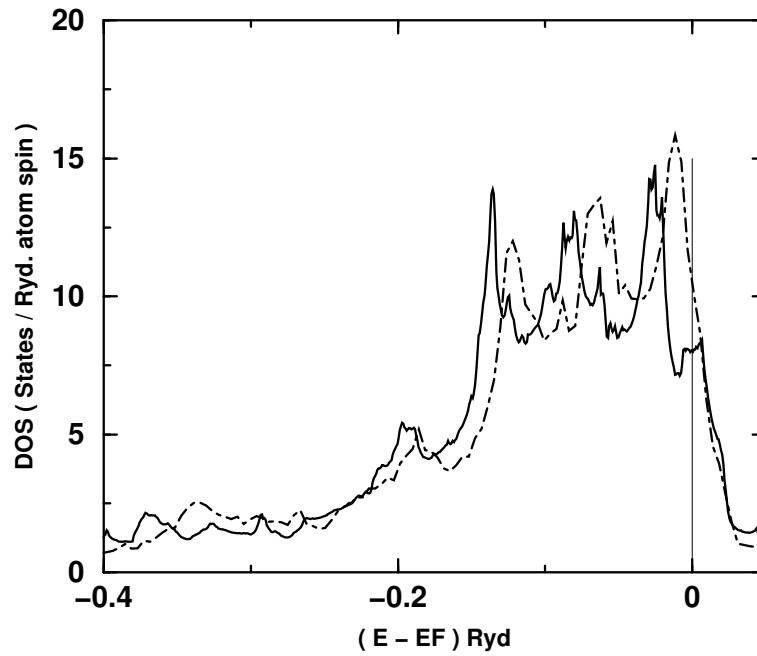


Figure 1. Paramagnetic density of states for d bands of Ni in ordered NiPd and NiPt alloys.

temperature we can argue that there magnetism should have an effect on phase stability of NiPd system reducing the value of order disorder transition temperature. Our calculation including magnetism indeed lowered the order disorder transition temperature.

Our calculations (with relativistic corrections) on CuAg shows a disorder to segregation transition temperature as 184°K. . This temperature in non relativistic case is slightly enhanced (201°K). Both the values are lower than experimental estimate (506°K).

### 3.3. Magnetic calculations in NiPd and NiPt alloys

In figure 1, we show paramagnetic density of states for d bands of Ni in ordered NiPd and NiPt alloys. It is seen that the d band of Ni is narrow in NiPd in comparison to NiPt which suggests that Ni in NiPd has higher magnetic moment than Ni in NiPt alloys.

To understand quantitatively the differences in the magnetic properties of these two systems, we have studied separation between majority and minority spin d band centres, separation between s and d band centres and spin polarized density of states in these NiPd and NiPt alloys.

**3.3.1. Separation Between Majority and Minority Spin d-band Centers :** The changes in the magnetic moments due to relativistic effects can be explained by examining the separation between majority spin and minority spin d-band centers of Ni ( $C_{d\uparrow}^{Ni}$  and  $C_{d\downarrow}^{Ni}$ ) in

NiPd and NiPt alloys.

We note that for NiPd relativistic corrections increase the separation of d-bands from 55.4 mRyd/atom to 57.3 mRyd/atom. This leads to a slight increase in the local magnetic moment from  $0.75 \mu_B/\text{atom}$  to  $0.76 \mu_B/\text{atom}$ . On the other hand, in NiPt the effect is to substantially reduce the d-band separation from 46.0 mRyd/atom to 21.9 mRyd/atom so that the local magnetic moment decreases from  $0.59 \mu_B/\text{atom}$  to  $0.30 \mu_B/\text{atom}$ .

We observe that the exchange-induced splitting of the d-band is higher in NiPd alloys for calculations done with and without relativistic corrections. The higher splitting leads to an increase in the local magnetic moment at the Ni site. It is interesting to note that the inclusion of relativistic corrections produces no net change in the exchange-induced splitting at the Ni site in NiPd. In NiPd due to these corrections the separation between d-band centers changes from 55.4 mRyd/atom to 57.3 mRyd/atom giving rise to  $0.75 \mu_B/\text{atom}$  to  $0.76 \mu_B/\text{atom}$ . On the other hand, in NiPt alloy we find that relativity substantially reduces the exchange-induced splitting at the Ni site leading to a decrease in the local magnetic moment of Ni. In NiPt the separation between d-band centers reduces from 46.0 mRyd/atom to 21.9 mRyd/atom due to relativity giving rise to the corresponding reduction in the local magnetic moment from  $0.59 \mu_B/\text{atom}$  to  $0.30 \mu_B/\text{atom}$ .

**3.3.2. Separation Between s and d Band Centers :** It is clear that the differences in the magnetic properties of NiPd and NiPt alloys are brought about by relativity through its effect on Pd and Pt atoms. We know that the most dominant effect of relativity is to lower the s potential. The lowering of s potential causes (i) the s-wavefunction to contract leading to a contraction of the lattice (ii) increased s-d hybridization which results in electron transfer from d to s. We see that the change in s-d separation is more in Pt than in Pd. The s-d separation for Pd in NiPd alloy changes from +59.0 mRyd to 7.6 mRyd, whereas for Pt in NiPt alloy, it changes from +84.0 mRyd to -199.1 mRyd. Thus the contraction of the s wavefunction of Pt and the subsequent s-d hybridization must be responsible for reducing the local magnetic moment at the Ni site in NiPt.

**3.3.3. Spin-Polarized Densities of States :** In figure 2 we show the spin-polarized DOS at the Ni site of disordered NiPd and NiPt alloys calculated with and without relativistic corrections. Since relativity is more important in NiPt than for NiPd, its effect on the DOS at the Ni site in NiPt is clearly seen. From the figure we see the substantial differences in the density of electrons at Fermi level in non relativistic and scalar relativistic cases of NiPt alloy but there is negligible difference in the case of NiPd.

**3.3.4. Magnetic moments :** From table 5 it is seen that magnetic moment calculated with and without relativistic corrections are similar in ordered as well as disordered NiPd alloys. However, the calculated average as well as local magnetic moments are

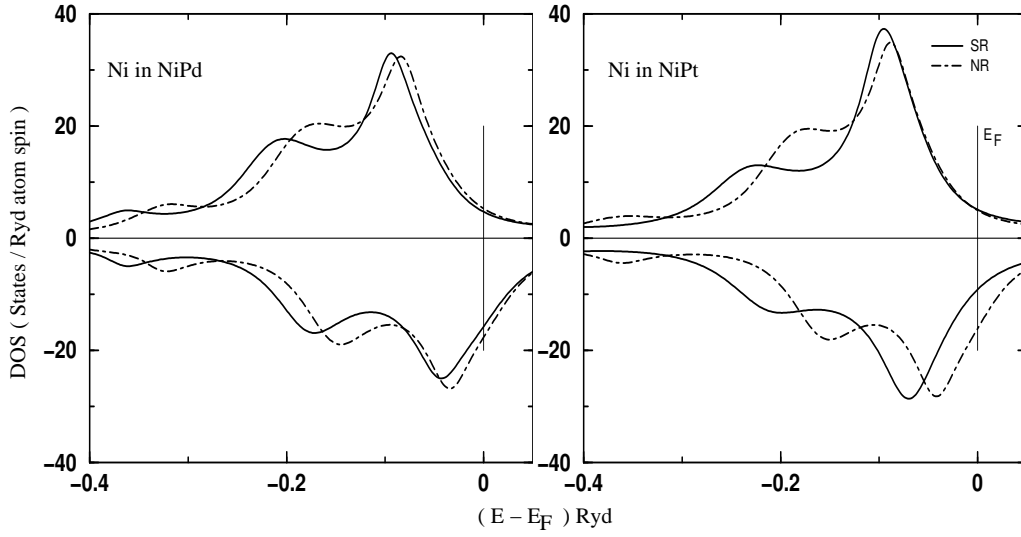


Figure 2. The spin-polarized densities of states of Ni, calculated non relativistically (NR) and scalar-relativistically (SR), in disordered NiPd and NiPt alloys.

quite different for ordered as well as disordered NiPt alloys with and without relativistic corrections. We find that the inclusion of relativity leads to a decrease in the magnetic moment at the Ni site by  $0.29 \mu_B/\text{atom}$  in NiPt alloy system. Our theoretically calculated disordered magnetic moment of NiPt with relativistic correction agrees with experimental estimates. Experimentally NiPt has got the effect of atomic short range order. With the inclusion of short range order effect we could get the magnetic moment of Ni further closer to the experimental value. The short range order effect in the magnetism of NiPt system is more important in the higher concentration of Pt (55% and 57%) which we described in our previous paper [5]. The calculated magnetic moments of Ni in NiPd alloy is very low ( $0.76 \text{ m Ryd/atom}$ ) in comparison to the diffuse scattering experiment ( $1.02 \text{ m Ryd/atom}$ ). This disagreement motivated us to suspect the effect of short range order on the magnetism of NiPd alloy. In order to check the possible short range order effect, we have checked the variation of total energy as a function of short range order parameter and found that the total energy decreases as short range order parameter goes from negative (ordering side) to positive (segregation side) confirming this system as an segregating system. We then checked the variation of magnetic moments as a function of SRO parameter and found that the magnetic moments of Ni increases by appreciable fraction. The moment of Pd decreases. These give rise to the increase of average magnetic moment. Calculated magnetic moments ( $0.90, 0.27$  and  $0.59 \mu_B/\text{atom}$  for Ni, Pd and average in NiPd) including the effect of segregation in this system agrees closely with the corresponding experimental values ( $1.02, 0.17$  and  $0.59 \mu_B/\text{atom}$  for Ni, Pd and average).

**3.3.5. Curie Temperature :** We have applied the Morin-Wolfarth model to calculate the Curie temperature as explained in the theoretical and computational details. Our Curie

Table 5. Calculated local and average magnetic moments in  $\mu_B$ /atom of NiPd and NiPt alloys. SRO and SRS denote short range order and short range segregation.

NiPd alloy				
Method	System	Ni site	Pd site	Average
TB-LMTO	Ordered (SR)	0.70	0.29	0.50
	Ordered (NR)	0.70	0.26	0.48
ASR	Disordered (SR)	0.76	0.31	0.54
	Disordered (NR)	0.75	0.28	0.51
	Disordered (SR) with SRS	0.90	0.27	0.59
Expt. [3]	Disordered	1.02	0.17	0.60
NiPt alloy				
Method	System	Ni site	Pt site	Average
TB-LMTO	Ordered (SR)	0.31	0.16	0.23
	Ordered (NR)	0.65	0.22	0.44
ASR	Disordered (SR)	0.30	0.11	0.20
	Disordered (NR)	0.59	0.21	0.40
	Disordered (SR) with SRO	0.27	0.14	0.21
Expt. [2]	Disordered	0.28	0.17	0.22

temperature calculation for NiPt with the relativistic correction ( $76^\circ\text{K}$ ) shows closer agreement with the experimental value ( $100^\circ\text{K}$ ). In contrast the Curie temperature without relativistic correction in the electronic structure calculation comes out ( $199^\circ\text{K}$ ) to be higher than the experimental estimate. This again justifies the fact that the relativistic effect plays a significant role in the correct estimation of magnetic transitions as well as magnetic moments. The calculated Curie temperatures with ( $245^\circ\text{K}$ ) and without relativistic correction ( $199^\circ\text{K}$ ) do not differ much as in the case of magnetic moments as explained above. The slightly higher value in relativistic case may be due to slightly higher (57.3 mRyd/atom) value of difference in d band centres than non relativistic case (55.4 mRyd/atom). These values of Curie temperatures with and without relativistic corrections do not actually match with experimental value ( $457^\circ\text{K}$ ). As we have explained above in the connection of magnetic moments, there is possibility of enhancement of magnetism due to the segregation tendency of this system. Our calculation taking into account this segregation effect through short range order parameter indeed shows the Curie temperature ( $345^\circ\text{K}$ ) closer to the experimental estimate. Therefore one can argue that in NiPd alloy system the atomic segregation tendency brings the strong enhancement in the magnetism.

#### 4. Conclusions

Our calculation for formation energies shows that NiPt and CuAu systems are stabilized by inclusion of relativistic effects. These effects ensure larger s-d hybridization by lowering s orbitals and raising d orbitals and lowers the strain and size mismatch in these alloys. Similar calculations show NiPd and CuAg to be unstable and there is very little effect of relativity in these systems. The pair interaction calculations in these systems show NiPt and CuAu have  $L1_0$  as the stable ground state structure as predicted from experiments. The positive value of first nearest neighbour pair energy in NiPd system even with the inclusion of relativistic effect indicates that this alloy tends to order, but experimentally it seems to remain disordered till low temperatures. Pair interaction calculation shows CuAg to be a segregating system as predicted from experiments.

Relativistic corrections ensure that the local magnetic moment of Ni is higher in NiPd than in NiPt consistent with experiment. The low value of local magnetic moment on Ni site in NiPt is facilitated by relativistic corrections again through lowering of the s potential of Pt, which leads to a contraction of the s wavefunction and an increase in s-d hybridization. We have obtained Curie temperature in NiPt reasonably comparable to the experimental estimate. Our Curie temperature calculation including short range segregation effect shows the enhancement in Curie temperature in the NiPd system, in better agreement with the experimental prediction than without it.

#### References

- [1] Wang L.G. and Zunger A., 2003 Phys. Rev. B 67, 092103
- [2] Parra R.E. and Medina R., 1980 Phys. Rev. B 22, 5460
- [3] Cable J.W. and Child H.R., 1970 Phys. Rev. B 1, 3809
- [4] Dahmani C.E., Cadeville, M.C., Sanchez J.M. and Moran-Lopez J.L. 1985, Phys. Rev. Lett. 55 1208
- [5] Paudyal D., Saha-Dasgupta T. and Mookerjee A., (2004) J. Phys.: Condens. Matter 16 2317
- [6] von Barth U. and Hedin L., 1972 J. Phys. C: Solid State Phys. 5 1629
- [7] Andersen O.K. and Jepsen O. 1984 Phys. Rev. Lett. 53 2581
- [8] Andersen O.K., Jepsen O. and Sob, Electronic Band Structure and Its Applications ed. M. Yussoufi. Lecture Notes in Physics 283, Springer (1987,1992)
- [9] Andersen O.K., Jepsen O. and Krier G., Lectures on Methods of Electronic Structure Calculations eds.: V. Kumar, O.K. Andersen, A. Mookerjee. Singapore, World Scientific, 1994.
- [10] Das G.P., Electronic Structure of Alloys, Surfaces and Clusters, Advances in Condensed Matter Science, Vol. 4, eds.: A. Mookerjee and D.D. Sharma, Taylor-Francis, 2003
- [11] V. Heine, Solid State Physics 35 (Academic Press, N.Y.) (1988)
- [12] Paudyal D., Saha-Dasgupta T. and Mookerjee A., 2003 J. Phys.: Condens. Matter 15 1029
- [13] Kanamori J., Kakehasi Y., J Physique Colloq. 38 C7-274 (1977)
- [14] Mookerjee A. and Prasad R., 1993 Phys. Rev. B 48 17724
- [15] Saha T., Dasgupta I. and Mookerjee A. 1994 Phys. Rev. B 50 13267
- [16] Ghosh S., Chaudhuri C.B., Sanyal B. and Mookerjee A., 2001 J. Magn. Magn. Mater. 234 100
- [17] Sanyal B., Biswas P.P., Mookerjee A., Das G.P., Salunke H. and Bhattacharya A.K., 1998 J. Phys.: Condens. Matter 10 5767

- [18] Biswas P. P., Sanyal B., Fakhruddin M., Halder A., Mukherjee A. and Ahmed M., 1995 J. Phys.: Condens. Matter 7 8569
- [19] Haydock R., Heine V. and Kelly M. J., 1972 J. Phys. C : Solid State Phys. 5 2845
- [20] Kudrnovsky J. and Drchal V., 1990 Phys. Rev. B 41 7515
- [21] Mohn P. H. and Wolfarth E. P. 1987 J. Phys. F 17 2421
- [22] Gunnarsson O. 1976 J. Phys. F 6 587
- [23] Gersdorff R. 1962 J. Phys. Radium 23 726
- [24] Ghosh S., Das N. and Mukherjee A., 1999 J. Phys.: Condens. Matter 9 10701
- [25] Ghosh S. D., Ph.D. Thesis, Jadavpur University, (2000)